PHYSICAL REVIEW D **108,** L031105 (2023)

Letter

Study of $\Lambda_c^+ \to \Lambda\mu^+\nu_\mu$ and test of lepton flavor universality with $\Lambda_c^+ \to \Lambda\ell^+\nu_\ell$ decays

M. Ablikim,[1] M. N. Achasov,[4,b] P. Adlarson,[75] X. C. Ai,[81] R. Aliberti,[35] A. Amoroso,[74a,74c] M. R. An,[39] Q. An,[71,58] Y. Bai,[57]
O. Bakina,[36] I. Balossino,[29a] Y. Ban,[46,g] H.-R. Bao,[63] V. Batozskaya,[1,44] K. Begzsuren,[32] N. Berger,[35] M. Berlowski,[44]
M. Bertani,[28a] D. Bettoni,[29a] F. Bianchi,[74a,74c] E. Bianco,[74a,74c] A. Bortone,[74a,74c] I. Boyko,[36] R. A. Briere,[5]
A. Brueggemann,[68] H. Cai,[76] X. Cai,[1,58] A. Calcaterra,[28a] G. F. Cao,[1,63] N. Cao,[1,63] S. A. Cetin,[62a] J. F. Chang,[1,58]
T. T. Chang,[77] W. L. Chang,[1,63] G. R. Che,[43] G. Chelkov,[36,a] C. Chen,[43] Chao Chen,[55] G. Chen,[1] H. S. Chen,[1,63]
M. L. Chen,[1,58,63] S. J. Chen,[42] S. L. Chen,[45] S. M. Chen,[61] T. Chen,[1,63] X. R. Chen,[31,63] X. T. Chen,[1,63] Y. B. Chen,[1,58]
Y. Q. Chen,[34] Z. J. Chen,[25,h] S. K. Choi,[10a] X. Chu,[43] G. Cibinetto,[29a] S. C. Coen,[3] F. Cossio,[74c] J. J. Cui,[50] H. L. Dai,[1,58]
J. P. Dai,[79] A. Dbeyssi,[18] R. E. de Boer,[3] D. Dedovich,[36] Z. Y. Deng,[1] A. Denig,[35] I. Denysenko,[36] M. Destefanis,[74a,74c]
F. De Mori,[74a,74c] B. Ding,[66,1] X. X. Ding,[46,g] Y. Ding,[40] Y. Ding,[34] J. Dong,[1,58] L. Y. Dong,[1,63] M. Y. Dong,[1,58,63] X. Dong,[76]
M. C. Du,[1] S. X. Du,[81] Z. H. Duan,[42] P. Egorov,[36,a] Y. H. Fan,[45] J. Fang,[1,58] S. S. Fang,[1,63] W. X. Fang,[1] Y. Fang,[1]
Y. Q. Fang,[1,58] R. Farinelli,[29a] L. Fava,[74b,74c] F. Feldbauer,[3] G. Felici,[28a] C. Q. Feng,[71,58] J. H. Feng,[59] K. Fischer,[69]
M. Fritsch,[3] C. D. Fu,[1] J. L. Fu,[63] Y. W. Fu,[1] H. Gao,[63] Y. N. Gao,[46,g] Yang Gao,[71,58] S. Garbolino,[74c] I. Garzia,[29a,29b]
P. T. Ge,[76] Z. W. Ge,[42] C. Geng,[59] E. M. Gersabeck,[67] A. Gilman,[69] K. Goetzen,[13] L. Gong,[40] W. X. Gong,[1,58] W. Gradl,[35]
S. Gramigna,[29a,29b] M. Greco,[74a,74c] M. H. Gu,[1,58] Y. T. Gu,[15] C. Y. Guan,[1,63] Z. L. Guan,[22] A. Q. Guo,[31,63] L. B. Guo,[41]
M. J. Guo,[50] R. P. Guo,[49] Y. P. Guo,[12,f] A. Guskov,[36,a] J. Gutierrez,[27] T. T. Han,[1] W. Y. Han,[39] X. Q. Hao,[19] F. A. Harris,[65]
K. K. He,[55] K. L. He,[1,63] F. H. H. Heinsius,[3] C. H. Heinz,[35] Y. K. Heng,[1,58,63] C. Herold,[60] T. Holtmann,[3] P. C. Hong,[12,f]
G. Y. Hou,[1,63] X. T. Hou,[1,63] Y. R. Hou,[63] Z. L. Hou,[1] B. Y. Hu,[59] H. M. Hu,[1,63] J. F. Hu,[56,i] T. Hu,[1,58,63] Y. Hu,[1]
G. S. Huang,[71,58] K. X. Huang,[59] L. Q. Huang,[31,63] X. T. Huang,[50] Y. P. Huang,[1] T. Hussain,[73] N. Hüsken,[27,35]
N. in der Wiesche,[68] M. Irshad,[71,58] J. Jackson,[27] S. Jaeger,[3] S. Janchiv,[32] J. H. Jeong,[10a] Q. Ji,[1] Q. P. Ji,[19] X. B. Ji,[1,63]
X. L. Ji,[1,58] Y. Y. Ji,[50] X. Q. Jia,[50] Z. K. Jia,[71,58] H. J. Jiang,[76] P. C. Jiang,[46,g] S. S. Jiang,[39] T. J. Jiang,[16] X. S. Jiang,[1,58,63]
Y. Jiang,[63] J. B. Jiao,[50] Z. Jiao,[23] S. Jin,[42] Y. Jin,[66] M. Q. Jing,[1,63] X. M. Jing,[63] T. Johansson,[75] S. Kabana,[33]
N. Kalantar-Nayestanaki,[64] X. L. Kang,[9] X. S. Kang,[40] M. Kavatsyuk,[64] B. C. Ke,[81] V. Khachatryan,[27] A. Khoukaz,[68]
R. Kiuchi,[1] R. Kliemt,[13] O. B. Kolcu,[62a] B. Kopf,[3] M. Kuessner,[3] A. Kupsc,[44,75] W. Kühn,[37] J. J. Lane,[67] P. Larin,[18]
A. Lavania,[26] L. Lavezzi,[74a,74c] T. T. Lei,[71,58] Z. H. Lei,[71,58] H. Leithoff,[35] M. Lellmann,[35] T. Lenz,[35] C. Li,[47] C. Li,[43]
C. H. Li,[39] Cheng Li,[71,58] D. M. Li,[81] F. Li,[1,58] G. Li,[1] H. Li,[71,58] H. B. Li,[1,63] H. J. Li,[19] H. N. Li,[56,i] Hui Li,[43] J. R. Li,[61]
J. S. Li,[59] J. W. Li,[50] Ke Li,[1] L. J. Li,[1,63] L. K. Li,[1] Lei Li,[48] M. H. Li,[43] P. R. Li,[38,k] Q. X. Li,[50] S. X. Li,[12] T. Li,[50]
W. D. Li,[1,63] W. G. Li,[1] X. H. Li,[71,58] X. L. Li,[50] Xiaoyu Li,[1,63] Y. G. Li,[46,g] Z. J. Li,[59] Z. X. Li,[15] C. Liang,[42] H. Liang,[1,63]
H. Liang,[71,58] Y. F. Liang,[54] Y. T. Liang,[31,63] G. R. Liao,[14] L. Z. Liao,[50] Y. P. Liao,[1,63] J. Libby,[26] A. Limphirat,[60]
D. X. Lin,[31,63] T. Lin,[1] B. J. Liu,[1] B. X. Liu,[76] C. Liu,[34] C. X. Liu,[1] F. H. Liu,[53] Fang Liu,[1] Feng Liu,[6] G. M. Liu,[56,i]
H. Liu,[38,j,k] H. B. Liu,[15] H. M. Liu,[1,63] Huanhuan Liu,[1] Huihui Liu,[21] J. B. Liu,[71,58] J. Y. Liu,[1,63] K. Liu,[1] K. Y. Liu,[40]
Ke Liu,[22] L. Liu,[71,58] L. C. Liu,[43] Lu Liu,[43] M. H. Liu,[12,f] P. L. Liu,[1] Q. Liu,[63] S. B. Liu,[71,58] T. Liu,[12,f] W. K. Liu,[43]
W. M. Liu,[71,58] X. Liu,[38,j,k] Y. Liu,[81] Y. Liu,[38,j,k] Y. B. Liu,[43] Z. A. Liu,[1,58,63] Z. Q. Liu,[50] X. C. Lou,[1,58,63] F. X. Lu,[59]
H. J. Lu,[23] J. G. Lu,[1,58] X. L. Lu,[1] Y. Lu,[7] Y. P. Lu,[1,58] Z. H. Lu,[1,63] C. L. Luo,[41] M. X. Luo,[80] T. Luo,[12,f] X. L. Luo,[1,58]
X. R. Lyu,[63] Y. F. Lyu,[43] F. C. Ma,[40] H. Ma,[79] H. L. Ma,[1] J. L. Ma,[1,63] L. L. Ma,[50] M. M. Ma,[1,63] Q. M. Ma,[1] R. Q. Ma,[1,63]
X. Y. Ma,[1,58] Y. Ma,[46,g] Y. M. Ma,[31] F. E. Maas,[18] M. Maggiora,[74a,74c] S. Malde,[69] Q. A. Malik,[73] A. Mangoni,[28b]
Y. J. Mao,[46,g] Z. P. Mao,[1] S. Marcello,[74a,74c] Z. X. Meng,[66] J. G. Messchendorp,[13,64] G. Mezzadri,[29a] H. Miao,[1,63] T. J. Min,[42]
R. E. Mitchell,[27] X. H. Mo,[1,58,63] B. Moses,[27] N. Yu. Muchnoi,[4,b] J. Muskalla,[35] Y. Nefedov,[36] F. Nerling,[18,d]
I. B. Nikolaev,[4,b] Z. Ning,[1,58] S. Nisar,[11,l] Q. L. Niu,[38,j,k] W. D. Niu,[55] Y. Niu,[50] S. L. Olsen,[63] Q. Ouyang,[1,58,63]
S. Pacetti,[28b,28c] X. Pan,[55] Y. Pan,[57] A. Pathak,[34] P. Patteri,[28a] Y. P. Pei,[71,58] M. Pelizaeus,[3] H. P. Peng,[71,58] Y. Y. Peng,[38,j,k]
K. Peters,[13,d] J. L. Ping,[41] R. G. Ping,[1,63] S. Plura,[35] V. Prasad,[33] F. Z. Qi,[1] H. Qi,[71,58] H. R. Qi,[61] M. Qi,[42] T. Y. Qi,[12,f]
S. Qian,[1,58] W. B. Qian,[63] C. F. Qiao,[63] J. J. Qin,[72] L. Q. Qin,[14] X. S. Qin,[50] Z. H. Qin,[1,58] J. F. Qiu,[1] S. Q. Qu,[61]
C. F. Redmer,[35] K. J. Ren,[39] A. Rivetti,[74c] M. Rolo,[74c] G. Rong,[1,63] Ch. Rosner,[18] S. N. Ruan,[43] N. Salone,[44] A. Sarantsev,[36,c]
Y. Schelhaas,[35] K. Schoenning,[75] M. Scodeggio,[29a,29b] K. Y. Shan,[12,f] W. Shan,[24] X. Y. Shan,[71,58] J. F. Shangguan,[55]
L. G. Shao,[1,63] M. Shao,[71,58] C. P. Shen,[12,f] H. F. Shen,[1,63] W. H. Shen,[63] X. Y. Shen,[1,63] B. A. Shi,[63] H. C. Shi,[71,58]
J. L. Shi,[12] J. Y. Shi,[1] Q. Q. Shi,[55] R. S. Shi,[1,63] X. Shi,[1,58] J. J. Song,[19] T. Z. Song,[59] W. M. Song,[34,1] Y. J. Song,[12]
Y. X. Song,[46,g] S. Sosio,[74a,74c] S. Spataro,[74a,74c] F. Stieler,[35] Y. J. Su,[63] G. B. Sun,[76] G. X. Sun,[1] H. Sun,[63] H. K. Sun,[1]
J. F. Sun,[19] K. Sun,[61] L. Sun,[76] S. S. Sun,[1,63] T. Sun,[51,e] W. Y. Sun,[34] Y. Sun,[9] Y. J. Sun,[71,58] Y. Z. Sun,[1] Z. T. Sun,[50]
Y. X. Tan,[71,58] C. J. Tang,[54] G. Y. Tang,[1] J. Tang,[59] Y. A. Tang,[76] L. Y. Tao,[72] Q. T. Tao,[25,h] M. Tat,[69] J. X. Teng,[71,58]
V. Thoren,[75] W. H. Tian,[52] W. H. Tian,[59] Y. Tian,[31,63] Z. F. Tian,[76] I. Uman,[62b] Y. Wan,[55] S. J. Wang,[50] B. Wang,[1]
B. L. Wang,[63] Bo Wang,[71,58] C. W. Wang,[42] D. Y. Wang,[46,g] F. Wang,[72] H. J. Wang,[38,j,k] J. P. Wang,[50] K. Wang,[1,58]

2470-0010/2023/108(3)/L031105(10)

Published by the American Physical Society

L. L. Wang,[1] M. Wang,[50] Meng Wang,[1,63] N. Y. Wang,[63] S. Wang,[38,j,k] S. Wang,[12,f] T. Wang,[12,f] T. J. Wang,[43] W. Wang,[59]
W. Wang,[72] W. P. Wang,[71,58] X. Wang,[46,g] X. F. Wang,[38,j,k] X. J. Wang,[39] X. L. Wang,[12,f] Y. Wang,[61] Y. D. Wang,[45]
Y. F. Wang,[1,58,63] Y. L. Wang,[19] Y. N. Wang,[45] Y. Q. Wang,[1] Yaqian Wang,[17,1] Yi Wang,[61] Z. Wang,[1,58] Z. L. Wang,[72]
Z. Y. Wang,[1,63] Ziyi Wang,[63] D. Wei,[70] D. H. Wei,[14] F. Weidner,[68] S. P. Wen,[1] C. W. Wenzel,[3] U. Wiedner,[3] G. Wilkinson,[69]
M. Wolke,[75] L. Wollenberg,[3] C. Wu,[39] J. F. Wu,[1,8] L. H. Wu,[1] L. J. Wu,[1,63] X. Wu,[12,f] X. H. Wu,[34] Y. Wu,[71] Y. H. Wu,[55]
Y. J. Wu,[31] Z. Wu,[1,58] L. Xia,[71,58] X. M. Xian,[39] T. Xiang,[46,g] D. Xiao,[38,j,k] G. Y. Xiao,[42] S. Y. Xiao,[1] Y. L. Xiao,[12,f]
Z. J. Xiao,[41] C. Xie,[42] X. H. Xie,[46,g] Y. Xie,[50] Y. G. Xie,[1,58] Y. H. Xie,[6] Z. P. Xie,[71,58] T. Y. Xing,[1,63] C. F. Xu,[1,63] C. J. Xu,[59]
G. F. Xu,[1] H. Y. Xu,[66] Q. J. Xu,[16] Q. N. Xu,[30] W. Xu,[1] W. L. Xu,[66] X. P. Xu,[55] Y. C. Xu,[78] Z. P. Xu,[42] Z. S. Xu,[63] F. Yan,[12,f]
L. Yan,[12,f] W. B. Yan,[71,58] W. C. Yan,[81] X. Q. Yan,[1] H. J. Yang,[51,e] H. L. Yang,[34] H. X. Yang,[1] Tao Yang,[1] Y. Yang,[12,f]
Y. F. Yang,[43] Y. X. Yang,[1,63] Yifan Yang,[1,63] Z. W. Yang,[38,j,k] Z. P. Yao,[50] M. Ye,[1,58] M. H. Ye,[8] J. H. Yin,[1] Z. Y. You,[59]
B. X. Yu,[1,58,63] C. X. Yu,[43] G. Yu,[1,63] J. S. Yu,[25,h] T. Yu,[72] X. D. Yu,[46,g] C. Z. Yuan,[1,63] L. Yuan,[2] S. C. Yuan,[1] X. Q. Yuan,[1]
Y. Yuan,[1,63] Z. Y. Yuan,[59] C. X. Yue,[39] A. A. Zafar,[73] F. R. Zeng,[50] S. H. Zeng,[72] X. Zeng,[12,f] Y. Zeng,[25,h] Y. J. Zeng,[1,63]
X. Y. Zhai,[34] Y. C. Zhai,[50] Y. H. Zhan,[59] A. Q. Zhang,[1,63] B. L. Zhang,[1,63] B. X. Zhang,[1] D. H. Zhang,[43] G. Y. Zhang,[19]
H. Zhang,[71] H. C. Zhang,[1,58,63] H. H. Zhang,[59] H. H. Zhang,[34] H. Q. Zhang,[1,58,63] H. Y. Zhang,[1,58] J. Zhang,[59] J. Zhang,[81]
J. J. Zhang,[52] J. L. Zhang,[20] J. Q. Zhang,[41] J. W. Zhang,[1,58,63] J. X. Zhang,[38,j,k] J. Y. Zhang,[1] J. Z. Zhang,[1,63] Jianyu Zhang,[63]
L. M. Zhang,[61] L. Q. Zhang,[59] Lei Zhang,[42] P. Zhang,[1,63] Q. Y. Zhang,[39,81] Shuihan Zhang,[1,63] Shulei Zhang,[25,h]
X. D. Zhang,[45] X. M. Zhang,[1] X. Y. Zhang,[50] Y. Zhang,[69] Y. Zhang,[72] Y. T. Zhang,[81] Y. H. Zhang,[1,58] Yan Zhang,[71,58]
Yao Zhang,[1] Z. D. Zhang,[1] Z. H. Zhang,[1] Z. L. Zhang,[34] Z. Y. Zhang,[43] Z. Y. Zhang,[76] G. Zhao,[1] J. Y. Zhao,[1,63]
J. Z. Zhao,[1,58] Lei Zhao,[71,58] Ling Zhao,[1] M. G. Zhao,[43] R. P. Zhao,[63] S. J. Zhao,[81] Y. B. Zhao,[1,58] Y. X. Zhao,[31,63]
Z. G. Zhao,[71,58] A. Zhemchugov,[36,a] B. Zheng,[72] J. P. Zheng,[1,58] W. J. Zheng,[1,63] Y. H. Zheng,[63] B. Zhong,[41] X. Zhong,[59]
H. Zhou,[50] L. P. Zhou,[1,63] X. Zhou,[76] X. K. Zhou,[6] X. R. Zhou,[71,58] X. Y. Zhou,[39] Y. Z. Zhou,[12,f] J. Zhu,[43]
K. Zhu,[1] K. J. Zhu,[1,58,63] L. Zhu,[34] L. X. Zhu,[63] S. H. Zhu,[70] S. Q. Zhu,[42] T. J. Zhu,[12,f] W. J. Zhu,[12,f]
Y. C. Zhu,[71,58] Z. A. Zhu,[1,63] J. H. Zou,[1] and J. Zu[71,58]

(BESIII Collaboration)

[1] *Institute of High Energy Physics, Beijing 100049, People's Republic of China*
[2] *Beihang University, Beijing 100191, People's Republic of China*
[3] *Bochum Ruhr-University, D-44780 Bochum, Germany*
[4] *Budker Institute of Nuclear Physics SB RAS (BINP), Novosibirsk 630090, Russia*
[5] *Carnegie Mellon University, Pittsburgh, Pennsylvania 15213, USA*
[6] *Central China Normal University, Wuhan 430079, People's Republic of China*
[7] *Central South University, Changsha 410083, People's Republic of China*
[8] *China Center of Advanced Science and Technology, Beijing 100190, People's Republic of China*
[9] *China University of Geosciences, Wuhan 430074, People's Republic of China*
[10] *Chung-Ang University, Seoul, 06974, Republic of Korea*
[11] *COMSATS University Islamabad, Lahore Campus, Defence Road, Off Raiwind Road, 54000 Lahore, Pakistan*
[12] *Fudan University, Shanghai 200433, People's Republic of China*
[13] *GSI Helmholtzcentre for Heavy Ion Research GmbH, D-64291 Darmstadt, Germany*
[14] *Guangxi Normal University, Guilin 541004, People's Republic of China*
[15] *Guangxi University, Nanning 530004, People's Republic of China*
[16] *Hangzhou Normal University, Hangzhou 310036, People's Republic of China*
[17] *Hebei University, Baoding 071002, People's Republic of China*
[18] *Helmholtz Institute Mainz, Staudinger Weg 18, D-55099 Mainz, Germany*
[19] *Henan Normal University, Xinxiang 453007, People's Republic of China*
[20] *Henan University, Kaifeng 475004, People's Republic of China*
[21] *Henan University of Science and Technology, Luoyang 471003, People's Republic of China*
[22] *Henan University of Technology, Zhengzhou 450001, People's Republic of China*
[23] *Huangshan College, Huangshan 245000, People's Republic of China*
[24] *Hunan Normal University, Changsha 410081, People's Republic of China*
[25] *Hunan University, Changsha 410082, People's Republic of China*
[26] *Indian Institute of Technology Madras, Chennai 600036, India*
[27] *Indiana University, Bloomington, Indiana 47405, USA*
[28a] *INFN Laboratori Nazionali di Frascati, INFN Laboratori Nazionali di Frascati, I-00044, Frascati, Italy*

[28b]*INFN Laboratori Nazionali di Frascati, INFN Sezione di Perugia, I-06100, Perugia, Italy*
[28c]*INFN Laboratori Nazionali di Frascati, University of Perugia, I-06100, Perugia, Italy*
[29a]*INFN Sezione di Ferrara, INFN Sezione di Ferrara, I-44122, Ferrara, Italy*
[29b]*INFN Sezione di Ferrara, University of Ferrara, I-44122, Ferrara, Italy*
[30]*Inner Mongolia University, Hohhot 010021, People's Republic of China*
[31]*Institute of Modern Physics, Lanzhou 730000, People's Republic of China*
[32]*Institute of Physics and Technology, Peace Avenue 54B, Ulaanbaatar 13330, Mongolia*
[33]*Instituto de Alta Investigación, Universidad de Tarapacá, Casilla 7D, Arica 1000000, Chile*
[34]*Jilin University, Changchun 130012, People's Republic of China*
[35]*Johannes Gutenberg University of Mainz, Johann-Joachim-Becher-Weg 45, D-55099 Mainz, Germany*
[36]*Joint Institute for Nuclear Research, 141980 Dubna, Moscow region, Russia*
[37]*Justus-Liebig-Universitaet Giessen, II. Physikalisches Institut, Heinrich-Buff-Ring 16, D-35392 Giessen, Germany*
[38]*Lanzhou University, Lanzhou 730000, People's Republic of China*
[39]*Liaoning Normal University, Dalian 116029, People's Republic of China*
[40]*Liaoning University, Shenyang 110036, People's Republic of China*
[41]*Nanjing Normal University, Nanjing 210023, People's Republic of China*
[42]*Nanjing University, Nanjing 210093, People's Republic of China*
[43]*Nankai University, Tianjin 300071, People's Republic of China*
[44]*National Centre for Nuclear Research, Warsaw 02-093, Poland*
[45]*North China Electric Power University, Beijing 102206, People's Republic of China*
[46]*Peking University, Beijing 100871, People's Republic of China*
[47]*Qufu Normal University, Qufu 273165, People's Republic of China*
[48]*Renmin University of China, Beijing 100872, People's Republic of China*
[49]*Shandong Normal University, Jinan 250014, People's Republic of China*
[50]*Shandong University, Jinan 250100, People's Republic of China*
[51]*Shanghai Jiao Tong University, Shanghai 200240, People's Republic of China*
[52]*Shanxi Normal University, Linfen 041004, People's Republic of China*
[53]*Shanxi University, Taiyuan 030006, People's Republic of China*
[54]*Sichuan University, Chengdu 610064, People's Republic of China*
[55]*Soochow University, Suzhou 215006, People's Republic of China*
[56]*South China Normal University, Guangzhou 510006, People's Republic of China*
[57]*Southeast University, Nanjing 211100, People's Republic of China*
[58]*State Key Laboratory of Particle Detection and Electronics, Beijing 100049, Hefei 230026, People's Republic of China*
[59]*Sun Yat-Sen University, Guangzhou 510275, People's Republic of China*
[60]*Suranaree University of Technology, University Avenue 111, Nakhon Ratchasima 30000, Thailand*
[61]*Tsinghua University, Beijing 100084, People's Republic of China*
[62a]*Turkish Accelerator Center Particle Factory Group, Istinye University, 34010, Istanbul, Turkey*
[62b]*Turkish Accelerator Center Particle Factory Group, Near East University, Nicosia, North Cyprus, 99138, Mersin 10, Turkey*
[63]*University of Chinese Academy of Sciences, Beijing 100049, People's Republic of China*
[64]*University of Groningen, NL-9747 AA Groningen, The Netherlands*
[65]*University of Hawaii, Honolulu, Hawaii 96822, USA*
[66]*University of Jinan, Jinan 250022, People's Republic of China*
[67]*University of Manchester, Oxford Road, Manchester, M13 9PL, United Kingdom*
[68]*University of Muenster, Wilhelm-Klemm-Strasse 9, 48149 Muenster, Germany*
[69]*University of Oxford, Keble Road, Oxford OX13RH, United Kingdom*
[70]*University of Science and Technology Liaoning, Anshan 114051, People's Republic of China*
[71]*University of Science and Technology of China, Hefei 230026, People's Republic of China*
[72]*University of South China, Hengyang 421001, People's Republic of China*
[73]*University of the Punjab, Lahore-54590, Pakistan*
[74a]*University of Turin and INFN, University of Turin, I-10125, Turin, Italy*
[74b]*University of Turin and INFN, University of Eastern Piedmont, I-15121, Alessandria, Italy*
[74c]*University of Turin and INFN, INFN, I-10125, Turin, Italy*
[75]*Uppsala University, Box 516, SE-75120 Uppsala, Sweden*
[76]*Wuhan University, Wuhan 430072, People's Republic of China*

[77]*Xinyang Normal University, Xinyang 464000, People's Republic of China*
[78]*Yantai University, Yantai 264005, People's Republic of China*
[79]*Yunnan University, Kunming 650500, People's Republic of China*
[80]*Zhejiang University, Hangzhou 310027, People's Republic of China*
[81]*Zhengzhou University, Zhengzhou 450001, People's Republic of China*

(Received 5 June 2023; accepted 17 July 2023; published 18 August 2023)

The study of the Cabibbo-favored semileptonic decay $\Lambda_c^+ \to \Lambda\mu^+\nu_\mu$ is reported using 4.5 fb^{-1} of e^+e^- annihilation data collected at center-of-mass energies ranging from 4.600 to 4.699 GeV. The branching fraction of the decay is measured to be $\mathcal{B}(\Lambda_c^+ \to \Lambda\mu^+\nu_\mu) = (3.48 \pm 0.14_{\mathrm{stat}} \pm 0.10_{\mathrm{syst}})\%$, 3 times more precise than the prior world average result. Tests of lepton flavor universality using $\Lambda_c^+ \to \Lambda\ell^+\nu_\ell$ ($\ell = e$, μ) decays are reported for the first time, based on measurements of the differential decay rates and the forward-backward asymmetries in separate four-momentum transfer regions. The results are compatible with Standard Model predictions. Furthermore, we improve the determination of the form-factor parameters in $\Lambda_c^+ \to \Lambda\ell^+\nu_\ell$ decays, which provide stringent tests and calibration for lattice quantum chromodynamics calculations.

DOI: 10.1103/PhysRevD.108.L031105

Semileptonic (SL) decays play a critical role in the determination of the Cabibbo-Kobayashi-Maskawa (CKM) matrix [1] elements which are fundamental parameters of the Standard Model (SM). The SM predicts that electroweak interactions have identical strengths for all three different lepton generations, which is known as lepton flavor universality (LFU). In recent years, tests of LFU show some hints of tension with SM predictions in both tree-level $b \to c\ell'\nu_{\ell'}$ ($\ell' = \tau, e, \mu$) transitions [2–10] and flavor-changing neutral current $b \to s\ell^+\ell^-$ ($\ell = e, \mu$) transitions [11–17]. Thus far, the experimental results on the combination of $\mathcal{R}(D)$ and $\mathcal{R}(D^*)$ show a discrepancy with respect to the SM prediction of about 3.4σ [18]. Measurements of $\mathcal{R}(K^{(*)})$ differed from the SM prediction by about 3.1σ [17] previously but this has recently decreased to 0.2σ [19]. Since violation of LFU would be a clear sign of new physics, further tests of LFU in other SL decays of heavy quarks are well motivated. The Cabibbo-favored decays $\Lambda_c^+ \to \Lambda\ell^+\nu_\ell$, the dominant Λ_c^+ SL decays [2], provide an ideal platform to test LFU via the e- and μ-modes, by measuring the ratios of their differential decay rates in separate four-momentum transfer regions. In addition, the angular distribution and the polarization effects in $\Lambda_c^+ \to \Lambda\ell^+\nu_\ell$ decays have received more and more attention in recent years [20–28]. Various asymmetrical parameters that characterize the angular dependence of the decay distributions are also accessible. In particular, the forward-backward asymmetry in the lepton system (A_{FB}^{ℓ}), which is the least sensitive to uncertainties of the form factors (FFs) parametrizing the hadronic matrix elements, can provide a critical test of LFU [20]. The forward-backward asymmetry in the hadronic $p\pi^-$ system (A_{FB}^{p}) can be used to extract the longitudinal polarization of the Λ baryon and the decay asymmetry parameter α_{Λ_c} [29,30]. Therefore, a model-independent measurement of these angular observables and decay rates is of great interest to test various theoretical calculations [20–28] and LFU. Furthermore, in the SM, the time-reversal (T) asymmetry in $\Lambda_c^+ \to \Lambda\ell^+\nu_\ell$ is zero due to the absence of a weak phase in

---

[a]Also at the Moscow Institute of Physics and Technology, Moscow 141700, Russia.

[b]Also at the Novosibirsk State University, Novosibirsk, 630090, Russia.

[c]Also at the NRC "Kurchatov Institute," PNPI, 188300, Gatchina, Russia.

[d]Also at Goethe University Frankfurt, 60323 Frankfurt am Main, Germany.

[e]Also at Key Laboratory for Particle Physics, Astrophysics and Cosmology, Ministry of Education; and Shanghai Key Laboratory for Particle Physics and Cosmology; Institute of Nuclear and Particle Physics, Shanghai 200240, People's Republic of China.

[f]Also at Key Laboratory of Nuclear Physics and Ion-beam Application (MOE) and Institute of Modern Physics, Fudan University, Shanghai 200443, People's Republic of China.

[g]Also at State Key Laboratory of Nuclear Physics and Technology, Peking University, Beijing 100871, People's Republic of China.

[h]Also at School of Physics and Electronics, Hunan University, Changsha 410082, China.

[i]Also at Guangdong Provincial Key Laboratory of Nuclear Science, Institute of Quantum Matter, South China Normal University, Guangzhou 510006, China.

[j]Also at MOE Frontiers Science Center for Rare Isotopes, Lanzhou University, Lanzhou 730000, People's Republic of China.

[k]Also at Lanzhou Center for Theoretical Physics, Lanzhou University, Lanzhou 730000, People's Republic of China.

[l]Also at the Department of Mathematical Sciences, IBA, Karachi 75270, Pakistan.

the $\Lambda_c^+ \to \Lambda$ transition [24,31]. Hence, measuring the T asymmetry in $\Lambda_c^+ \to \Lambda\ell^+\nu_\ell$ is a clean way to search for new physics with a CP-violating phase beyond the SM. Throughout this Letter, charge-conjugate modes are implied unless explicitly noted.

This Letter presents an improved measurement of the branching fraction (BF) of $\Lambda_c^+ \to \Lambda\mu^+\nu_\mu$ [32]. We also report the first measurement of the differential decay rates and the forward-backward asymmetries for $\Lambda_c^+ \to \Lambda\ell^+\nu_\ell$ decays in the full kinematic range as well as individual four-momentum transfer regions. Using these observables, we provide the first test on LFU using $\Lambda_c^+ \to \Lambda\ell^+\nu_\ell$ decays. The forward-backward asymmetries are obtained from both the current muonic sample and a reexamination of the previous electronic sample of Ref. [33]. Furthermore, an improved measurement of FFs in $\Lambda_c^+ \to \Lambda\ell^+\nu_\ell$ decays in comparison to Ref. [33] is provided, by analyzing the data of $\Lambda_c^+ \to \Lambda\mu^+\nu_\mu$ and $\Lambda_c^+ \to \Lambda e^+\nu_e$ decays simultaneously. The datasets are collected at the center-of-mass energies $\sqrt{s} = 4.600$, 4.612, 4.628, 4.641, 4.661, 4.682, and 4.699 GeV, with a total integrated luminosity of 4.5 fb^{-1} [34,35]. At these energies, no additional hadrons accompanying the $\Lambda^+\bar{\Lambda}_c^-$ pairs are kinematically allowed.

Details about the BESIII detector design and performance are provided in Refs. [36–38]. Monte Carlo (MC) simulations for the signal and background samples are similar to those described in Ref. [33]. We select "single tag" (ST) and "double tag" (DT) samples to measure the absolute BF of $\Lambda_c^+ \to \Lambda\mu^+\nu_\mu$ decay. Single tag decays are $\bar{\Lambda}_c^-$ baryons reconstructed from their final state particles in one of the 14 hadronic decays used in Ref. [39]. Double tag decays are events with a ST and a Λ_c^+ baryon candidate reconstructed as $\Lambda\mu^+\nu_\mu$. The ST $\bar{\Lambda}_c^-$ signal candidates are identified using the beam constrained mass

$$M_{\rm BC} = \sqrt{(\sqrt{s}/2)^2 - |\vec{p}_{\bar{\Lambda}_c^-}|^2},$$

where $\vec{p}_{\bar{\Lambda}_c^-}$ is the measured momentum of the ST $\bar{\Lambda}_c^-$ candidate. A kinematic variable $\Delta E = E_{\rm beam} - E_{\bar{\Lambda}_c^-}$ is required to improve the signal significance for ST $\bar{\Lambda}_c^-$ baryons. The ΔE requirements, $M_{\rm BC}$ distributions, and their ST yields are documented in Ref. [39]. The total ST yield in all datasets is $N^{\rm ST} = 122,268 \pm 474$, where the uncertainty is statistical only.

Candidates for the signal mode $\Lambda_c^+ \to \Lambda\mu^+\nu_\mu$ are selected from the remaining tracks recoiling against the ST $\bar{\Lambda}_c^-$ candidates. The $\Lambda \to p\pi^-$ candidate is selected with the same criteria as those used in the ST procedures [33]. The μ candidate is identified with the combined information of dE/dx measured in the multilayer drift chamber, time of flight, and the energy measured in the electromagnetic calorimeter (EMC), and is required to satisfy $\mathcal{L}_\mu > 0.001$, $\mathcal{L}_\mu > \mathcal{L}_e$, and $\mathcal{L}_\mu > \mathcal{L}_K$, where $\mathcal{L}_\mu$, $\mathcal{L}_e$, and $\mathcal{L}_K$ are the particle identification probabilities for a muon, electron, and kaon, respectively. Studies of inclusive MC samples show that the backgrounds are dominated by $\Lambda_c^+ \to \Lambda\pi^+$, $\Sigma^0\pi^+$, and $\Lambda\pi^+\pi^0$. Backgrounds from $\Lambda_c^+ \to \Lambda\pi^+$ and $\Lambda_c^+ \to \Sigma^0\pi^+$ are rejected by a requirement on the $\Lambda\mu^+$ invariant mass, $M_{\Lambda\mu^+} < 2.12$ GeV. The background from $\Lambda_c^+ \to \Lambda\pi^+\pi^0$ is suppressed by requiring the maximum energy of all unused photon clusters, $E_{\gamma\,\rm max}$, to be less than 0.25 GeV and the deposited energy for the muon candidate in the EMC to be less than 0.30 GeV. Since the neutrino is not detected, we employ the kinematic variable $U_{\rm miss} = E_{\rm miss} - |\vec{p}_{\rm miss}|$ to obtain information on the neutrino, where $E_{\rm miss}$ and $\vec{p}_{\rm miss}$ are the missing energy and momentum, respectively, carried by the neutrino, as inferred from energy-momentum conservation.

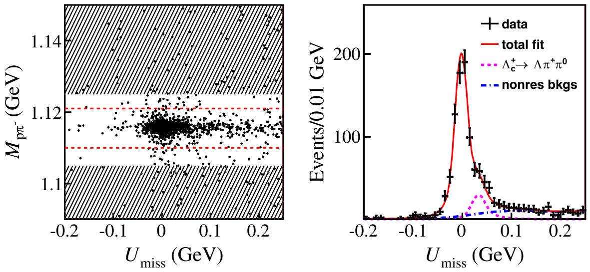

FIG. 1. Left: the $M_{p\pi^-}$ versus $U_{\rm miss}$ distribution for the $\Lambda_c^+ \to \Lambda\mu^+\nu_\mu$ candidates. The area between the dashed lines denotes the Λ signal region and the hatched areas indicate the Λ sideband regions. Right: projected $U_{\rm miss}$ distribution within the Λ signal region together with the fit.

Figure 1 (left) shows the distribution of $M_{p\pi^-}$ versus $U_{\rm miss}$ for the $\Lambda_c^+ \to \Lambda\mu^+\nu_\mu$ candidates in data. A cluster of the events is located around the intersection of the Λ and $\Lambda\mu^+\nu_\mu$ signal region. Requiring $M_{p\pi^-}$ to be within the Λ signal region, we project the distribution onto the $U_{\rm miss}$ axis, as shown in Fig. 1 (right). To obtain the number of signal events, the $U_{\rm miss}$ distribution is fitted with a signal function which consists of a Gaussian to describe the core of the $U_{\rm miss}$ distribution and two power law tails to account for initial and final state radiations [40,41]. A MC-simulated background shape is used to describe the peaking background from $\Lambda_c^+ \to \Lambda\pi^+\pi^0$, and a MC-simulated nonresonant background shape is used to describe the continuous background. In the fit, the size of peaking background from $\Lambda_c^+ \to \Lambda\pi^+\pi^0$ is fixed according to the BF $\mathcal{B}(\Lambda_c^+ \to \Lambda\pi^+\pi^0)$ [2] and the simulated efficiency [42]. From the fit, we obtain the yield of $\Lambda_c^+ \to \Lambda\mu^+\nu_\mu$ decay $N^{\rm DT} = 752 \pm 31$, where the uncertainty is statistical only.

The absolute BF for $\Lambda_c^+ \to \Lambda\mu^+\nu_\mu$ is determined by

$$\mathcal{B}(\Lambda_c^+ \to \Lambda\mu^+\nu_\mu) = \frac{N^{\rm DT}}{N^{\rm ST} \times \varepsilon_{\rm semi}}, \tag{1}$$

where $\varepsilon_{\rm semi} = 0.1767$ is the average efficiency for detecting the $\Lambda_c^+ \to \Lambda\mu^+\nu_\mu$ decay in ST events [33,40]. Inserting the values of N^{DT}, N^{ST}, and $\varepsilon_{\mathrm{semi}}$ into Eq. (1), we measure $\mathcal{B}(\Lambda_c^+ \to \Lambda\mu^+\nu_\mu) = (3.48 \pm 0.14 \pm 0.10)\%$, where the first uncertainty is statistical, and the second is systematic uncertainty described below.

With the DT technique, the BF measurement is insensitive to the systematic uncertainties of the ST selection. The remaining systematic uncertainties in the BF measurement are described as follows. The uncertainties of the μ^+ tracking and particle identification efficiencies are determined to be 0.3% and 0.5% studied using $e^+e^- \to \gamma\mu^+\mu^-$ events. The uncertainty due to Λ reconstruction is determined to be 0.2% studied with $J/\psi \to pK^-\bar{\Lambda}$ and $J/\psi \to \Lambda\bar{\Lambda}$ control samples. The uncertainty associated with the simulation of the SL signal model is estimated to be 1.0% by varying the input form-factor parameters by 1 standard deviation as determined in this work. Further systematic uncertainties include fit to the U_{miss} distribution (1.8%) estimated by using alternative signal shapes and background shapes, requirements on $M_{\Lambda\mu^+}$ (0.8%), $E_{\gamma\,\mathrm{max}}$ (0.6%), and deposited energy (0.8%), the quoted BF for $\Lambda \to p\pi^-$ (0.8%) [2], the MC sample size (0.8%), and the ST yield (1.0%). Adding these contributions in quadrature gives a total systematic uncertainty of 2.9% for the $\mathcal{B}(\Lambda_c^+ \to \Lambda\mu^+\nu_\mu)$ measurement.

The partial decay rate of $\Lambda_c^+ \to \Lambda\ell^+\nu_\ell$ is measured by analyzing the $\ell^+\nu_\ell$ mass-squared (q^2) distribution. The candidates of $\Lambda_c^+ \to \Lambda e^+\nu_e$ are selected as in Ref. [33]. The q^2 distributions of $\Lambda_c^+ \to \Lambda\ell^+\nu_\ell$ candidates are divided into seven bins of [0, 0.20), [0.20, 0.40), [0.40, 0.60), [0.60, 0.80), [0.80, 1.00), [1.00, 1.20), and [1.20, q^2_{max}) GeV^2, where $q^2_{\mathrm{max}} = (M_{\Lambda_c} - M_\Lambda)^2$ and $M_{\Lambda_{(c)}}$ is the mass of $\Lambda_{(c)}$. The measured partial decay rate in the ith q^2 bin, $\Delta\Gamma_i$, is determined by

$$\Delta\Gamma_i = \int_i \frac{d\Gamma}{dq^2}dq^2 = \sum_{j=1}^{N_{\mathrm{bins}}}(\epsilon^{-1})_{ij}N^j_{\mathrm{DT}}/(\tau_{\Lambda_c} \times N^{\mathrm{ST}}), \quad (2)$$

where τ_{Λ_c} is the lifetime of Λ_c^+ [2] and ϵ_{ij} is the efficiency matrix to describe the reconstruction efficiency of SL decays and migration effects across q^2 bins [43,44]. The SL signal yield observed in the jth q^2 bin N^j_{DT} is obtained from a fit to the corresponding U_{miss} distribution. The measured differential decay rates, $\Delta\Gamma_i/\Delta q^2$, for decays $\Lambda_c^+ \to \Lambda e^+\nu_e$ and $\Lambda_c^+ \to \Lambda\mu^+\nu_\mu$ as well as their ratios $\mathcal{R}^{\mu/e}_{\Delta\Gamma/\Delta q^2}$ in each bin are shown in Fig. 2 (left). The distributions of the $d\Gamma/dq^2$ and $\mathcal{R}^{\mu/e}_{\Delta\Gamma/\Delta q^2}$ as a function of q^2 calculated using the FFs measured in this work (described later) and those predicted by lattice quantum chromodynamics (LQCD) [28] are also shown in Fig. 2 (left). The ratios $\mathcal{R}^{\mu/e}_{\Delta\Gamma/\Delta q^2}$ measured in different q^2 intervals are consistent with LQCD calculation within 1 standard deviation, which suggests that no evidence for violation of LFU is found.

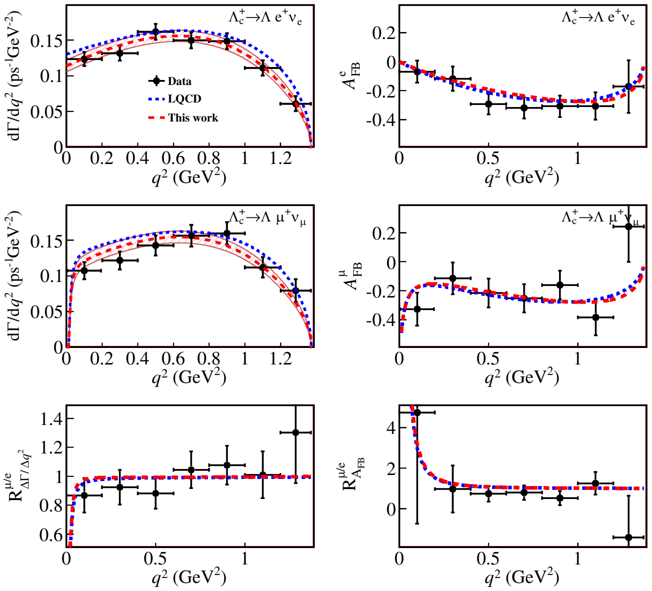

FIG. 2. Top row: measurements of (left) $\Delta\Gamma/\Delta q^2$ and (right) A^ℓ_{FB} vs q^2 for $\Lambda_c^+ \to \Lambda e^+\nu_e$. Middle row: the same quantities for $\Lambda_c^+ \to \Lambda\mu^+\nu_\mu$. Bottom row: the ratios of the above, $\mathcal{R}^{\mu/e}$. The dots with error bars are data, where statistical and systematic uncertainties are both included. The red dash-dotted curves show the derived values using the FFs measured in this work, while the blue dashed curves show those predicted by LQCD [28]. The bands show the total uncertainties of $d\Gamma/dq^2$ using the FFs measured in this work.

The model-independent forward-backward asymmetries of both the lepton system, $A^\ell_{\mathrm{FB}}(q^2)$, and of the $p\pi^-$ system, $A^p_{\mathrm{FB}}(q^2)$ are also measured with $\Lambda_c^+ \to \Lambda\ell^+\nu_\ell$ candidates. The definition of forward-backward asymmetry $A^{\ell,p}_{\mathrm{FB}}(q^2)$ follows [20,21]

$$A^{\ell,p}_{\mathrm{FB}}(q^2) = \frac{\int_0^1 \frac{d^2\Gamma}{dq^2 d\cos\theta_{\ell,p}} d\cos\theta_{\ell,p} - \int_{-1}^0 \frac{d^2\Gamma}{dq^2 d\cos\theta_{\ell,p}} d\cos\theta_{\ell,p}}{\int_0^1 \frac{d^2\Gamma}{dq^2 d\cos\theta_{\ell,p}} d\cos\theta_{\ell,p} + \int_{-1}^0 \frac{d^2\Gamma}{dq^2 d\cos\theta_{\ell,p}} d\cos\theta_{\ell,p}}, \quad (3)$$

where $d^2\Gamma/(dq^2 d\cos\theta_{\ell,p})$ is the two-dimensional differential rate, and θ_ℓ is the angle between the lepton (e^+/μ^+) direction and the $\ell^+\nu_\ell$ system direction in the Λ_c^+ rest frame, and θ_p is the angle between the proton and the Λ direction also in the Λ_c^+ rest frame. To measure $A^{\ell,p}_{\mathrm{FB}}(q^2)$, the q^2 distributions of the SL candidates are separated into two regions of $\cos\theta_{\ell,p} \in (0,1)$ and $\cos\theta_{\ell,p} \in (-1,0)$. With a similar procedure as applied in measuring the partial decay rate defined in Eq. (2), the $\Delta\Gamma_i/\Delta q^2$ within $\cos\theta_{\ell,p} \in (0,1)$ and $\cos\theta_{\ell,p} \in (-1,0)$ is measured for each q^2 bin. Then we extract the forward-backward asymmetries, $A^\ell_{\mathrm{FB}}(q^2)$ and $A^p_{\mathrm{FB}}(q^2)$, for each q^2 bin with

Eq. (3). The results for $A_{\mathrm{FB}}^{\ell}(q^2)$ of $\Lambda_c^+ \to \Lambda e^+\nu_e$ and $\Lambda_c^+ \to \Lambda\mu^+\nu_\mu$ as well as their ratios $\mathcal{R}_{A_{\mathrm{FB}}}^{\mu/e}$ are shown in Fig. 2 (right), where their dependences calculated with the FFs measured in this work and those predicted by LQCD [28] are also presented. Measurements of $\mathcal{R}_{A_{\mathrm{FB}}}^{\mu/e}$ in various q^2 bins also show no evidence for a violation of the LFU.

The $A_{\mathrm{FB}}^{p}(q^2)$ for $\Lambda_c^+ \to \Lambda e^+\nu_e$ and $\Lambda_c^+ \to \Lambda\mu^+\nu_\mu$ measured in each q^2 interval are shown in Fig. 3 (left). Using the relation

$$\alpha_{\Lambda_c}(q^2) = \frac{2}{\alpha_\Lambda}[A_{\mathrm{FB}}^{p}(q^2)], \tag{4}$$

where α_Λ is the $\Lambda \to p\pi^-$ decay asymmetry parameter [2], the model-independent decay asymmetry parameter α_{Λ_c} for $\Lambda_c^+ \to \Lambda\ell^+\nu_\ell$ in separate q^2 intervals is measured. Differences in α_{Λ_c} between the e- and μ-modes are expected at an order of 10^{-3} [20,21,24], indistinguishable with current statistics. Alternatively, their averaged value is determined in each q^2 interval as shown in Fig. 3 (right). This is the first model-independent determination of α_{Λ_c} as a function of q^2 distribution. In addition, we determined the value averaged over q^2 to be $\langle\alpha_{\Lambda_c}\rangle = -0.94 \pm 0.07_{\mathrm{stat}} \pm 0.03_{\mathrm{syst}}$.

We also measure the T asymmetry parameter $\mathcal{T}_p$ defined by [24]

$$\mathcal{T}_p = \frac{[(\int_{-\pi}^{0} - \int_{0}^{\pi})d\chi][(\int_{0}^{1} - \int_{-1}^{0})d\cos\theta_p]\Gamma_{\chi,\cos\theta_p}^{\ell}}{\alpha_\Lambda \Gamma^{\ell}},$$

where Γ^{ℓ} is the total decay rate and $\Gamma_{\chi,\cos\theta_p}^{\ell}$ is the two-dimensional decay rate as a function of χ and $\cos\theta_p$ distributions in $\Lambda_c^+ \to \Lambda\ell^+\nu_\ell$, where χ is the acoplanarity angle between the Λ and W^+ decay planes. We measure $\mathcal{T}_p(\Lambda_c^+ \to \Lambda e^+\nu_e) = -0.021 \pm 0.041_{\mathrm{stat}} \pm 0.001_{\mathrm{syst}}$ and $\mathcal{T}_p(\Lambda_c^+ \to \Lambda\mu^+\nu_\mu) = 0.068 \pm 0.055_{\mathrm{stat}} \pm 0.002_{\mathrm{syst}}$. The two results are consistent with zero, as predicted from the SM [24], with no indication of new physics in $\Lambda_c^+ \to \Lambda\ell^+\nu_\ell$ decays.

To improve experimental precision of the FF parameters in the $\Lambda_c^+ \to \Lambda$ transition, the candidates from $\Lambda_c^+ \to \Lambda\mu^+\nu_\mu$ in this work and $\Lambda_c^+ \to \Lambda e^+\nu_e$ obtained in Ref. [33] are analyzed simultaneously. The differential decay rate of $\Lambda_c^+ \to \Lambda\ell^+\nu_\ell$ depends on four kinematic variables: q^2, helicity angles θ_p and θ_ℓ' [45], and the acoplanarity angle χ. The differential decay rate described in terms of helicity amplitudes $H_{\lambda_\Lambda\lambda_W}$ is [29,30,46]

$$\begin{aligned}\frac{d^4\Gamma}{dq^2 d\cos\theta_\ell' d\cos\theta_p d\chi} = {}& \frac{G_F^2|V_{cs}|^2}{2(2\pi)^4}\cdot\frac{Pq^2(1-m_\ell^2/q^2)^2}{24M_{\Lambda_c}^2}\bigg\{\frac{3}{8}(1-\cos\theta_\ell')^2|H_{\frac{1}{2}1}|^2(1+\alpha_\Lambda\cos\theta_p) \\ & + \frac{3}{8}(1+\cos\theta_\ell')^2|H_{-\frac{1}{2}-1}|^2(1-\alpha_\Lambda\cos\theta_p) \\ & + \frac{3}{4}\sin^2\theta_\ell'[|H_{\frac{1}{2}0}|^2(1+\alpha_\Lambda\cos\theta_p)+|H_{-\frac{1}{2}0}|^2(1-\alpha_\Lambda\cos\theta_p)] + \frac{3}{2\sqrt{2}}\alpha_\Lambda\cos\chi\sin\theta_\ell'\sin\theta_p \\ & \times[(1-\cos\theta_\ell')H_{-\frac{1}{2}0}H_{\frac{1}{2}1}+(1+\cos\theta_\ell')H_{\frac{1}{2}0}H_{-\frac{1}{2}-1}] + \mathcal{H}_{m_\ell^2}\bigg\},\end{aligned} \tag{5}$$

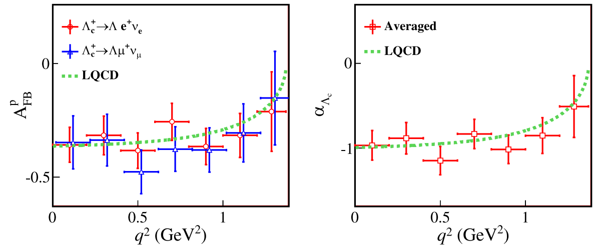

FIG. 3. Measurements of (left) $A_{\mathrm{FB}}^{p}(q^2)$ for $\Lambda_c^+ \to \Lambda\ell^+\nu_\ell$ and (right) the averaged α_{Λ_c} of the e- and μ-modes in each q^2 interval. The dots with error bars are data, where statistical and systematic uncertainties are both included. The dashed curve shows the derived values predicted by LQCD [28]. In drawing the blue dots, the bin-center value of q^2 is shifted manually by 0.02 GeV^2 to avoid overlap.

where m_ℓ is the lepton mass. The definitions of the variables $H_{\lambda_\Lambda\lambda_W}$, G_F, $|V_{cs}|$, and P follow those in Ref. [33]. The detailed expression of $\mathcal{H}_{m_\ell^2}$ is documented in the Supplemental Material [47].

The helicity amplitudes of vector and axial-vector components, $H_{\lambda_\Lambda\lambda_W}^{V}$ and $H_{\lambda_\Lambda\lambda_W}^{A}$, parametrized in Eq. (5) are related to six FFs by [28]

$$\begin{aligned} H_{\frac{1}{2}1}^{V/A} &= \sqrt{2Q_\mp}f_\perp/g_\perp(q^2), \\ H_{\frac{1}{2}0}^{V/A} &= \sqrt{Q_\mp/q^2}f_+/g_+(q^2)(M_{\Lambda_c} \pm M_\Lambda), \\ H_{\frac{1}{2}t}^{V/A} &= \sqrt{Q_\pm/q^2}f_0/g_0(q^2)(M_{\Lambda_c} \mp M_\Lambda), \end{aligned} \tag{6}$$

where the scalar helicity component is denoted by $\lambda_W = t$ and $Q_\pm = (M_{\Lambda_c} \pm M_\Lambda)^2 - q^2$. The FFs $f_0(q^2)$ and $g_0(q^2)$

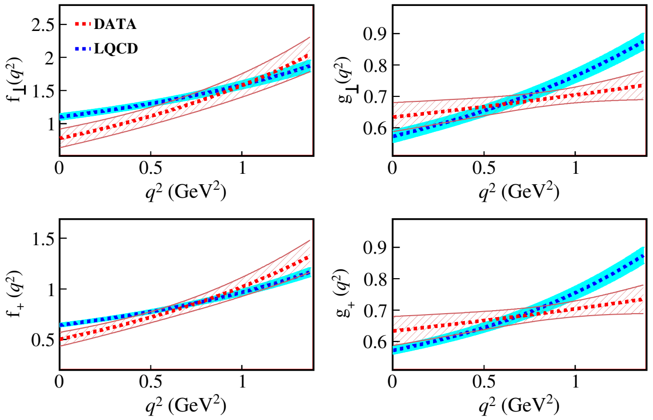

FIG. 4. Comparison of form factors with LQCD calculations. The bands show the total uncertainties.

have a small contribution to the decay rate and hence are difficult to determine. Hence the shapes of $f_0(q^2)$ and $g_0(q^2)$ are fixed according to a LQCD calculation [28]. The definitions of the independent free parameters formed in the other four form factors, $f_{\perp,+}(q^2)$ and $g_{\perp,+}(q^2)$, follow Ref. [33]. An additional constraint, $g_+(q^2_{\max}) = g_\perp(q^2_{\max})$, introduced by end point relations for baryons [48] is taken into account, which results in $g_+(q^2) = g_\perp(q^2)$ as we neglect the differences of the slope parameters ($\alpha_1^{g_{+,\perp}}$) between $g_+(q^2)$ and $g_\perp(q^2)$. Therefore, the five independent free parameters, $a_0^{g_\perp}$, $\alpha_1^{g_\perp}$, $\alpha_1^{f_\perp}$, $r_{f_+} = a_0^{f_+}/a_0^{g_\perp}$, $r_{f_\perp} = a_0^{f_\perp}/a_0^{g_\perp}$, are introduced to describe the FFs.

A four-dimensional maximum-likelihood fit is performed to the variables q^2, $\cos\theta'_\ell$, $\cos\theta_p$, and χ within the $U_{\rm miss}$ signal regions defined by $(-0.06, 0.06)$ GeV for both $\Lambda_c^+ \to \Lambda e^+\nu_e$ and $\Lambda_c^+ \to \Lambda\mu^+\nu_\mu$ decays. In order to determine the parameter $a_0^{g_\perp}$ from the fit, the differential decay rate of $\Lambda_c^+ \to \Lambda\mu(e)^+\nu_{\mu(e)}$ is constrained by the BF of $\Lambda_c^+ \to \Lambda\mu(e)^+\nu_{\mu(e)}$ measured in this work (Ref. [33]) and the Λ_c^+ lifetime [2] using the relation

$$\int_{m_\ell^2}^{q^2_{\max}} \frac{d\Gamma(\Lambda_c^+ \to \Lambda\ell^+\nu_\ell)}{dq^2} dq^2 = \frac{\mathcal{B}(\Lambda_c^+ \to \Lambda\ell^+\nu_\ell)}{\tau_{\Lambda_c}}. \qquad (7)$$

The projections of the fit onto q^2, $\cos\theta'_\ell$, $\cos\theta_p$, and χ, as well as the fitted form-factor parameters of $a_0^{g_\perp}$, $\alpha_1^{g_\perp}$, $\alpha_1^{f_\perp}$, r_{f_+}, and $r_{f_\perp}$ are shown in the Supplemental Material [47]. Using a treatment similar to Ref. [33], the systematic uncertainties in $a_0^{g_\perp}$, $\alpha_1^{g_\perp}$, $\alpha_1^{f_\perp}$, r_{f_+}, and $r_{f_\perp}$ are estimated to be 0.8%, 6.3%, 2.2%, 1.3%, and 5.8%, respectively. In comparison to Ref. [33], the precision in measuring $a_0^{g_\perp}$, $\alpha_1^{g_\perp}$, r_{f_+}, and $r_{f_\perp}$ is improved by 25%, 11%, 22%, and 43%, respectively. The comparisons to the LQCD calculations [28] are shown in Fig. 4. The dependence of the measured FFs show different kinematic behavior compared to the LQCD calculations, especially for the slopes of these four FFs.

In summary, we report an improved measurement of the absolute BF of the $\Lambda_c^+ \to \Lambda\mu^+\nu_\mu$ decay, $\mathcal{B}(\Lambda_c^+ \to \Lambda\mu^+\nu_\mu) = (3.48 \pm 0.14 \pm 0.10)\%$, by analyzing 4.5 fb^{-1} data collected at center-of-mass energies ranging from 4.600 to 4.699 GeV at BESIII. This work supersedes our previous measurement [32] and improves the precision of the world average value by a factor of 3. Comparisons to the theoretical predictions are also shown in Table I. The predicted BFs in Refs. [20,49] differ by more than 2 standard deviations from the measured $\mathcal{B}(\Lambda_c^+ \to \Lambda\mu^+\nu_\mu)$. Thus, our measurement disfavors these predictions at a confidence level of more than 95%. Combining with $\mathcal{B}(\Lambda_c^+ \to \Lambda e^+\nu_e) = (3.56 \pm 0.11 \pm 0.07)\%$ in Ref. [33], we determine the ratio $\mathcal{B}(\Lambda_c^+ \to \Lambda\mu^+\nu_\mu)/\mathcal{B}(\Lambda_c^+ \to \Lambda e^+\nu_e) = 0.98 \pm 0.05_{\rm stat} \pm 0.03_{\rm syst}$, which is consistent with the value 0.97 as predicted by LQCD [28]. The ratio of the two BFs in different four-momentum

TABLE I. Comparisons of $\mathcal{B}(\Lambda_c^+ \to \Lambda\mu^+\nu_\mu)$ (in %), $\langle\alpha_{\Lambda_c}\rangle$, $\langle A^e_{\rm FB}\rangle$, and $\langle A^\mu_{\rm FB}\rangle$ from theories and measurement.

	$\mathcal{B}(\Lambda_c^+ \to \Lambda\mu^+\nu_\mu)$	$\langle\alpha_{\Lambda_c}\rangle$	$\langle A^e_{\rm FB}\rangle$	$\langle A^\mu_{\rm FB}\rangle$
CQM [20]	2.69	−0.87	−0.2	−0.21
RQM [21]	3.14	−0.86	−0.209	−0.242
CQM(HONR) [49]	4.25			
NRQM [50]	3.72			
HBM [24]	3.67 ± 0.23	−0.826	−0.176(5)	−0.143(6)
LQCD [28]	3.69 ± 0.22	−0.874(10)	−0.201(6)	−0.169(7)
LCSR [51]	3.0 ± 0.3			
SU(3) [25]	3.6 ± 0.4	−0.86(4)		
LFCQM [27]	3.21 ± 0.85	−0.97(3)		
MBM [27]	3.38	−0.83		
LFQM [22]	3.90 ± 0.73	−0.87(9)	0.20(5)	0.16(4)
LFCQM [26]	3.40 ± 1.02	−0.97(3)		
SU(3) [52]	3.45 ± 0.30			
This work	3.48 ± 0.17	−0.94(8)	−0.24(3)	−0.22(4)

transfer regions is also studied, and no evidence for the LFU violation is found.

In addition, the model-independent lepton forward-backward asymmetries $A_{\mathrm{FB}}^{e,\mu}(q^2)$ as well as their ratios are measured for the first time. Their average values are determined to be $\langle A_{\mathrm{FB}}^{e}\rangle = -0.24 \pm 0.03_{\mathrm{stat}} \pm 0.01_{\mathrm{syst}}$ and $\langle A_{\mathrm{FB}}^{\mu}\rangle = -0.22 \pm 0.04_{\mathrm{stat}} \pm 0.01_{\mathrm{syst}}$, respectively. The measured $\langle A_{\mathrm{FB}}^{e}\rangle$ and $\langle A_{\mathrm{FB}}^{\mu}\rangle$ are consistent with the predictions in Refs. [20,21,24,28], but clearly differ from the predictions in Ref. [22]. The detailed comparisons are shown in Table I. Investigations of $\mathcal{R}_{A_{\mathrm{FB}}}^{\mu/e}$ in different four-momentum transfer regions show no evidence for the LFU violation. As a first measurement of the forward-backward asymmetries in the $p\pi^-$ system, we determine the averaged values $\langle A_{\mathrm{FB}}^{p}\rangle = -0.33 \pm 0.03_{\mathrm{stat}} \pm 0.01_{\mathrm{syst}}$ and $\langle A_{\mathrm{FB}}^{p}\rangle = -0.37 \pm 0.04_{\mathrm{stat}} \pm 0.01_{\mathrm{syst}}$ for $\Lambda_c^+ \to \Lambda e^+\nu_e$ and $\Lambda_c^+ \to \Lambda\mu^+\nu_\mu$, respectively. Ignoring the negligible predicted difference between the e- and μ-modes, the $\langle \alpha_{\Lambda_c}\rangle$ is determined to be $-0.94 \pm 0.07_{\mathrm{stat}} \pm 0.03_{\mathrm{syst}}$, which is consistent with the theoretical predictions in Refs. [20–28] and the model-dependent measurement by CLEO [30]. Our measurements of the T asymmetry parameters, $\mathcal{T}_p(\Lambda_c^+ \to \Lambda e^+\nu_e) = -0.021 \pm 0.041_{\mathrm{stat}} \pm 0.001_{\mathrm{syst}}$ and $\mathcal{T}_p(\Lambda_c^+ \to \Lambda\mu^+\nu_\mu) = 0.068 \pm 0.055_{\mathrm{stat}} \pm 0.002_{\mathrm{syst}}$, are consistent with zero as predicted in the SM. Furthermore, our results on the form factors provide more stringent tests of and calibration for LQCD calculations of $\Lambda_c^+ \to \Lambda\ell^+\nu_\ell$ decays, which are important for both charmed baryon decays [53,54] and Λ_b decays [22,55–61].

The BESIII Collaboration thanks the staff of BEPCII and the IHEP computing center for their strong support. This work is supported in part by National Key R&D Program of China under Contracts No. 2020YFA0406400 and No. 2020YFA0406300; National Natural Science Foundation (NSFC) of China under Contracts No. 11635010, No. 11735014, No. 11835012, No. 11935015, No. 11935016, No. 11935018, No. 11961141012, No. 12022510, No. 12025502, No. 12035009, No. 12035013, No. 12061131003, No. 12192260, No. 12192261, No. 12192262, No. 12192263, No. 12192264, and No. 12192265; the Chinese Academy of Sciences (CAS) Large-Scale Scientific Facility Program; the CAS Center for Excellence in Particle Physics; Joint Large-Scale Scientific Facility Funds of the NSFC and CAS under Contract No. U1832207; CAS Key Research Program of Frontier Sciences under Contracts No. QYZDJ-SSW-SLH003 and No. QYZDJ-SSW-SLH040; 100 Talents Program of CAS; The Institute of Nuclear and Particle Physics and Shanghai Key Laboratory for Particle Physics and Cosmology; ERC under Contract No. 758462; European Union's Horizon 2020 research and innovation program under Marie Sklodowska-Curie grant agreement under Contract No. 894790; German Research Foundation DFG under Contracts No. 443159800 and No. 455635585, Collaborative Research Center CRC 1044, FOR5327, GRK 2149; Istituto Nazionale di Fisica Nucleare, Italy; Ministry of Development of Turkey under Contract No. DPT2006K-120470; National Research Foundation of Korea under Contract No. NRF-2022R1A2C1092335; National Science and Technology Fund of Mongolia; National Science Research and Innovation Fund via the Program Management Unit for Human Resources & Institutional Development, Research and Innovation of Thailand under Contract No. B16F640076; Polish National Science Centre under Contract No. 2019/35/O/ST2/02907; The Royal Society, UK under Contract No. DH160214; The Swedish Research Council; U.S. Department of Energy under Contract No. DE-FG02-05ER41374.

[1] M. Kobayashi and T. Maskawa, Prog. Theor. Phys. **49**, 652 (1973).

[2] R. L. Workman *et al.* (Particle Data Group), Prog. Theor. Exp. Phys. **2022**, 083C01 (2022).

[3] J. P. Lees *et al.* (*BABAR* Collaboration), Phys. Rev. Lett. **109**, 101802 (2012).

[4] J. P. Lees *et al.* (*BABAR* Collaboration), Phys. Rev. D **88**, 072012 (2013).

[5] M. Huschle *et al.* (Belle Collaboration), Phys. Rev. D **92**, 072014 (2015).

[6] Y. Sato *et al.* (Belle Collaboration), Phys. Rev. D **94**, 072007 (2016).

[7] R. Aaij *et al.* (LHCb Collaboration), Phys. Rev. Lett. **115**, 111803 (2015).

[8] S. Hirose *et al.* (Belle Collaboration), Phys. Rev. Lett. **118**, 211801 (2017).

[9] R. Aaij *et al.* (LHCb Collaboration), Phys. Rev. D **97**, 072013 (2018).

[10] S. Hirose *et al.* (Belle Collaboration), Phys. Rev. Lett. **120**, 171802 (2018).

[11] J. P. Lees *et al.* (*BABAR* Collaboration), Phys. Rev. D **86**, 032012 (2012).

[12] R. Aaij *et al.* (LHCb Collaboration), J. High Energy Phys. 06 (2017) 108.

[13] R. Aaij *et al.* (LHCb Collaboration), J. High Energy Phys. 08 (2017) 055.

[14] R. Aaij *et al.* (LHCb Collaboration), Phys. Rev. Lett. **122**, 191801 (2019).

[15] R. Aaij *et al.* (LHCb Collaboration), J. High Energy Phys. 05 (2020) 040.
[16] S. Choudhury *et al.* (Belle Collaboration), J. High Energy Phys. 03 (2021) 105.
[17] R. Aaij *et al.* (LHCb Collaboration), Nat. Phys. **18**, 277 (2022).
[18] Y. Amhis *et al.* (HFLAV Collaboration), Eur. Phys. J. C **81**, 226 (2021).
[19] R. Aaij *et al.* (LHCb Collaboration), arXiv:2212.09152; arXiv:2212.09153.
[20] T. Gutsche, M. A. Ivanov, J. G. Körner, V. E. Lyubovitskij, and P. Santorelli, Phys. Rev. D **93**, 034008 (2016).
[21] R. N. Faustov and V. O. Galkin, Eur. Phys. J. C **76**, 628 (2016).
[22] Y. S. Li, X. Liu, and F. S. Yu, Phys. Rev. D **104**, 013005 (2021).
[23] M. Golz, G. Hiller, and T. Magorsch, J. High Energy Phys. 09 (2021) 208.
[24] C. Q. Geng, X. N. Jin, and C. W. Liu, Phys. Rev. D **107**, 033008 (2023).
[25] C. Q. Geng, C. W. Liu, T. H. Tsai, and S. W. Yeh, Phys. Lett. B **792**, 214 (2019).
[26] C. Q. Geng, C. W. Liu, and T. H. Tsai, Phys. Rev. D **103**, 054018 (2021).
[27] C. Q. Geng, Chong-Chung Lih, C. W. Liu, and T. H. Tsai, Phys. Rev. D **101**, 094017 (2020).
[28] S. Meinel, Phys. Rev. Lett. **118**, 082001 (2017).
[29] J. G. Körner and M. Krämer, Phys. Lett. B **275**, 495 (1992).
[30] J. W. Hinson *et al.* (CLEO Collaboration), Phys. Rev. Lett. **94**, 191801 (2005).
[31] C. Q. Geng, X. N. Jin, and C. W. Liu, Phys. Rev. D **106**, 053006 (2022).
[32] M. Ablikim *et al.* (BESIII Collaboration), Phys. Lett. B **767**, 42 (2017).
[33] M. Ablikim *et al.* (BESIII Collaboration), Phys. Rev. Lett. **129**, 231803 (2022).
[34] M. Ablikim *et al.* (BESIII Collaboration), Chin. Phys. C **39**, 093001 (2015).
[35] M. Ablikim *et al.* (BESIII Collaboration), Chin. Phys. C **46**, 113003 (2022).
[36] M. Ablikim *et al.* (BESIII Collaboration), Nucl. Instrum. Methods Phys. Res., Sect. A **614**, 345 (2010).
[37] K. X. Huang *et al.*, Nucl. Sci. Tech. **33**, 142 (2022).
[38] M. Ablikim *et al.* (BESIII Collaboration), Chin. Phys. C **44**, 040001 (2020).
[39] M. Ablikim *et al.* (BESIII Collaboration), Phys. Rev. D **106**, 112010 (2022).
[40] M. Ablikim *et al.* (BESIII Collaboration), Phys. Rev. Lett. **115**, 221805 (2015).
[41] J. Y. Ge *et al.* (CLEO Collaboration), Phys. Rev. D **79**, 052010 (2009).
[42] M. Ablikim *et al.* (BESIII Collaboration), J. High Energy Phys. 12 (2022) 033.
[43] M. Ablikim *et al.* (BESIII Collaboration), Phys. Rev. Lett. **124**, 241802 (2020).
[44] M. Ablikim *et al.* (BESIII Collaboration), Phys. Rev. D **101**, 112002 (2020).
[45] It should be noted that $\theta'_\ell = \pi - \theta_\ell$.
[46] A. Kadeer, J. G. Körner, and U. Moosbrugger, Eur. Phys. J. C **59**, 27 (2009).
[47] See Supplemental Material at http://link.aps.org/supplemental/10.1103/PhysRevD.108.L031105 for the detailed expression for $\mathcal{H}_{m_\ell^2}$, projection plots of the kinematic variables for $\Lambda_c^+ \to \Lambda e^+ \nu_e$ and $\Lambda_c^+ \to \Lambda \mu^+ \nu_\mu$ decays, and the fitted form-factor parameters from the maximum-likelihood fits.
[48] G. Hiller and R. Zwicky, J. High Energy Phys. 11 (2021) 073.
[49] M. Pervin, W. Roberts, and S. Capstick, Phys. Rev. C **72**, 035201 (2005).
[50] M. M. Hussain and W. Roberts, Phys. Rev. D **95**, 053005 (2017); **95**, 099901 (2017).
[51] Y. L. Liu, M. Q. Huang, and D. W. Wang, Phys. Rev. D **80**, 074011 (2009).
[52] X. G. He, F. Huang, W. Wang, and Z. P. Xing, Phys. Lett. B **823**, 136765 (2021).
[53] Q. A. Zhang, H. Hua, F. Huang, R. Li, Y. Li, C. D. Lü, P. Sun, W. Wang, and Y. B. Yang, Chin. Phys. C **46**, 011002 (2022).
[54] X. G. He, F. Huang, W. Wang, and Z. P. Xing, Phys. Lett. B **823**, 136765 (2021).
[55] S. Meinel and G. Rendon, Phys. Rev. D **105**, 054511 (2022).
[56] K. Azizi, M. Bayar, Y. Sarac, and H. Sundu, Phys. Rev. D **80**, 096007 (2009).
[57] T. Gutsche, M. A. Ivanov, J. G. Körner, V. E. Lyubovitskij, and P. Santorelli, Phys. Rev. D **90**, 114033 (2014); **94**, 059902(E) (2016).
[58] T. Feldmann and M. W. Y. Yip, Phys. Rev. D **85**, 014035 (2012); **86**, 079901(E) (2012).
[59] W. Detmold, C. J. David Lin, S. Meinel, and M. Wingate, Phys. Rev. D **88**, 014512 (2013).
[60] W. Detmold, C. Lehner, and S. Meinel, Phys. Rev. D **92**, 034503 (2015).
[61] W. Detmold and S. Meinel, Phys. Rev. D **93**, 074501 (2016).